CDK8 and CDK19 act redundantly to control the CFTR pathway in the intestinal epithelium

Susana Prieto, Geronimo Dubra, Lucie Angevin, Ana Bella Aznar, Alain Camasses, Christina Begon-Pescia, Nelly Pirot, François Gerbe, Philippe Jay, Liliana Krasinska, et al.

▶ **To cite this version:**

Susana Prieto, Geronimo Dubra, Lucie Angevin, Ana Bella Aznar, Alain Camasses, et al.. CDK8 and CDK19 act redundantly to control the CFTR pathway in the intestinal epithelium. 17eme Journees Canceropole GSO, Nov 2021, Carcassonne, France. hal-03866091

HAL Id: hal-03866091
https://hal.science/hal-03866091

Submitted on 22 Nov 2022

HAL is a multi-disciplinary open access archive for the deposit and dissemination of scientific research documents, whether they are published or not. The documents may come from teaching and research institutions in France or abroad, or from public or private research centers.

L'archive ouverte pluridisciplinaire **HAL**, est destinée au dépôt et à la diffusion de documents scientifiques de niveau recherche, publiés ou non, émanant des établissements d'enseignement et de recherche français ou étrangers, des laboratoires publics ou privés.

CDK8 and CDK19 act redundantly to control the CFTR pathway in the intestinal epithelium

Susana Prieto[1,2], Geronimo Dubra[1,2], Lucie Angevin[1,2], Ana Bella Aznar[1,2], Alain Camasses[1,2], Christina Begon-Pescia[1,6], Nelly Pirot[4,5], François Gerber[2,3], Philippe Jay[2,3], Liliana Krasinska[1,2] and Daniel Fisher[1,2]

[1]IGMM, University of Montpellier, CNRS, Inserm, Montpellier, France.
[2]Equipe Labellisée LIGUE 2018, Ligue Nationale Contre le Cancer, Paris, France.
[3]IGF, University of Montpellier, CNRS, Inserm, Montpellier, France.
[4]IRCM, University of Montpellier, ICM, INSERM, Montpellier, France
[5]BioCampus, RHEM, University of Montpellier, CNRS, INSERM, Montpellier, France
[6]Current address: LPHI, University of Montpellier, Montpellier, France

Abstract

CDK8 and CDK19 form a highly conserved cyclin-dependent kinase subfamily that binds to and inhibits the essential transcription complex, Mediator, and is thought to also activate gene expression by phosphorylating the C-terminal domain (CTD) of RNA polymerase II. Cells lacking either CDK8 or CDK19 are viable and have somewhat limited transcriptional alterations, but how they regulate expression of different genes has not been explained, and whether one of the two kinases must be expressed to allow cell differentiation is unknown. Here, we find that CDK8 and CDK19 are largely functionally redundant for tissue-specific gene expression. Genetic deletion of CDK8 in mice does not affect normal intestinal homeostasis and efficient tumourigenesis, and CDK8 is not required *in vivo* in cells lacking the main PolII CTD kinase, CDK7. Individual knockout of genes encoding CDK8 or CDK19 in intestinal organoids has only limited effects on gene expression due to their extensive functional redundancy in control of gene expression. Surprisingly, although their combined deletion in organoids reduces long-term proliferative capacity, it is not lethal and allows differentiation. Nevertheless, either CDK8 or CDK19 is required to maintain expression of the Cystic Fibrosis Transmembrane conductance Regulator (CFTR) pathway. In double mutant organoids, the CFTR pathway is downregulated, leading to mucus accumulation and increased secretion by goblet cells. Pharmacological inhibition indicates that expression and function of the CFTR pathway is dependent on CDK8/19 kinase activity. We conclude that expression of the Mediator kinases is not essential for cell proliferation and differentiation, but they cooperate to regulate tissue-specific transcriptional programmes.

Fig 1and 2. CDK8 knockout does not affect adult mouse intestine homeostasis

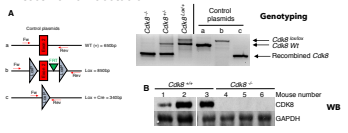

Fig 1. Mouse *Cdk8* conditional knockout by Lox/Cre targeting of exon 2. (A) Left, scheme representing the control plasmids (a, b, and c) for WT, floxed and recombined *Cdk8* exon 2. Right, genotyping of *Cdk8* exon 2 in the mouse intestinal epithelium. All mice were treated with Tamoxifen to induce recombination of the Lox^P sites. The recombined fragment appears as a 340 bp band in the *Cdk8* $^{-/-}$ and *Cdk8* $^{+/-}$ mice (*Villin*Cre^{ERT2} recombinase-positive), and is absent in the *Cdk8* $^{Lox/+}$ mouse that does not contain the *Villin*Cre^{ERT2} gene. **(B)** WB analysis of mouse intestine epithelium showing the absence of CDK8 protein 2 months after Tamoxifen feeding. GAPDH protein was used as loading control.

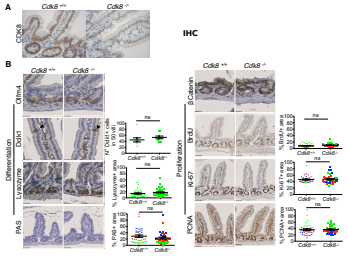

Fig. 2. (A) Immunohistochemical staining of CKD8 in mouse small intestines collected two months after tamoxifen treatment. **(B)** Analysis of cell differentiation (left) and proliferation (right) in the intestine after CDK8 deletion (as in A). Olfm4, Lysozyme, PAS and Dclk1 staining was used to reveal, respectively, stem, Paneth, goblet and tuft cells. β-Catenin staining allows detection of cancer cells (cytoplasmic vs nuclear localisation). Cell proliferation was assessed by PCNA, Ki-67 and BrdU (after 1h pulse) staining. Scatter plots represent the percentage of the area stained by each antibody (relative to the area occupied by hematoxylin). For Paneth cells, BrdU, PCNA and Ki67, only crypts were analysed. For goblet cells, crypts and villi were analysed. For Tuft cells quantification, Dclk1 positive cells were counted in 50 villi. Colour code depicts small intestine (green), proximal colon (blue), and distant colon (red). Mean ± SEM is shown. P-value of unpaired two-tailed t-test is indicated (ns, not significant; p > 0.05). Scale bars, 25μm (Olfm4, Lysozyme, Dclk1 and β-Catenin) and 50μm (PAS, BrdU, Ki-67 and PCNA).

Fig 3.
-No critical role for CDK8 in RNA-PolII C-Terminal Domain (CTD) phosphorylation.
-Low levels of CDK7 are sufficient for RNA-PolII CTD-phosphorylation

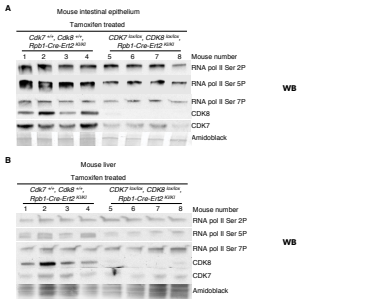

Fig 3. Effects of CDK8 and CDK7 knockout on RNA pol II CTD phosphorylation. WB analysis of the indicated proteins in mouse intestinal epithelium **(A)** or liver **(B)** samples from WT and *Cdk7* $^{lox/lox}$ *Cdk8* $^{lox/lox}$; *Rpb-Cre-Ert2* $^{KI/KI}$ mice after tamoxifen treatment. Amido-black staining was used as loading control.

Fig 4. CDK8 loss does not affect chemically-induced intestinal carcinogenesis.

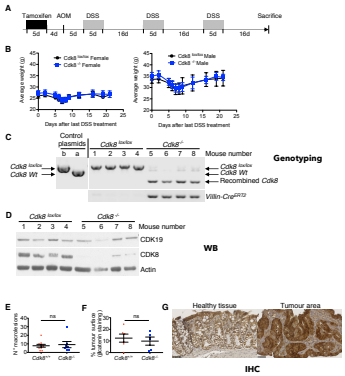

Fig 4. (A) Scheme showing the steps of the AOM/DSS carcinogenesis experiment. **(B)** Graphs showing the survival (left; n=6 in both groups) and male (right; n=5 in both groups) weight evolution over 21 days following the last DSS treatment. **(C)** Genotyping after AOM/DSS treatment confirms the recombination and loss of *Cdk8* exon 2 in colon tumors from *Cdk8* $^{-/-}$ mice. Control plasmids (a and b), are described in Fig 1A. **(D)** WB with the same colon tumour samples presented in (C). β-actin was used as the loading control. **(E)** Quantification of the number of neoplastic lesions (n = 10 for Cdk8 $^{+/+}$, and n = 7 for Cdk8 $^{-/-}$ mice). P-value of unpaired t-test is indicated: ns, not significant (p > 0.05). Mean ± SD is shown. **(F)** Quantification of the percentage of the colon surface occupied by tumours. Intestine samples were stained for β-Catenin, and tumour regions with nuclear β-Catenin localisation were quantified. Two-tailed p-value of unpaired t-test is indicated; ns, not significant (p > 0.05). Mean ± SD is shown. **(G)** Example of IHC with β-Catenin staining of tumour-free regions with membrane β-catenin localization *(left)* and tumour regions with nuclear β-catenin localisation *(right)*. Scale bars, 50μm.

Fig 5. CDK8 deletion does not prevent Apc-loss-dependent tumourigenesis in mouse intestine.

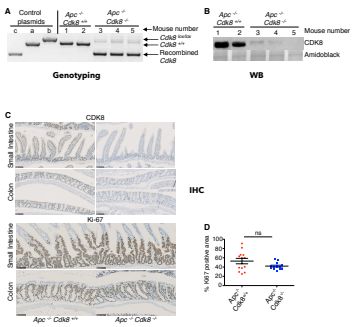

Fig 5. (A) Genotyping confirms the loss of *Cdk8* exon 2 in intestine epithelium from *Apc* $^{-/-}$*/Cdk8* $^{-/-}$ mice. Control plasmids (a, b and c) are described in Fig 1A. **(B)** WB with intestine epithelium samples from mice presented in (A) confirm the absence of CDK8 protein in *Cdk8* $^{-/-}$ mice. Amido-black staining was used as loading control. **(C)** IHC staining of CDK8 and Ki-67 in small intestine and colon samples from *Apc* $^{-/-}$*/Cdk8* $^{+/+}$ and *Apc* $^{-/-}$*/Cdk8* $^{-/-}$ mice. Scale bars, 100μm. **(D)** Quantification of the Ki-67 positive area (% of the total area of the intestine presenting positive staining, quantified using QuPath and Image J software; mean ± SD) in the Ki-67 IHC shown in (C). Ki-67 (n=16). Two-tailed p-value of unpaired t-test is indicated: ns, not significant (p > 0.05).

Fig 6. Amino acid sequence conservation of CDK8 and its paralogue CDK19 between different vertebrates.

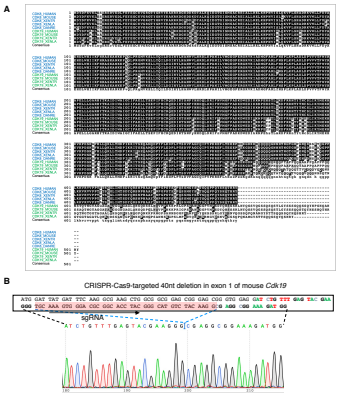

Fig 6. (A) Sequence alignment of Cdk8 (blue) and Cdk19 (green) proteins from: *Homo sapiens, Mus musculus, Xenopus tropicalis, Xenopus laevis, and Danio rerio*. Homologous sequences are black. The consensus (> 80%) is presented below the alignment. **(B)** Scheme indicating the fragment of *Cdk19* exon 1 removed by CRISPR-Cas9 (highlighted in red) in intestinal organoids. The arrow indicates the sequence of the sgRNA used. The sequence trace obtained after gene editing is presented below. The colour-code in the sequence in the box corresponds to the sequence trace.

Fig 7. Double CDK8/CDK19 knockout intestinal organoids show decreased cell proliferation.

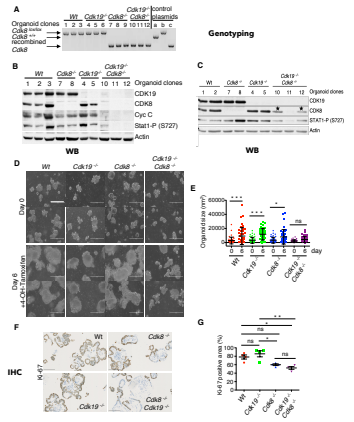

Fig. 7. (A) Genotyping confirms the loss of *Cdk8* exon 2 in *Cdk8* $^{-/-}$ and *Cdk8* $^{-/-}$*/Cdk19* $^{-/-}$ organoids after 7 days of OH-tamoxifen treatment. Control plasmids (a, b and c) are described in Fig 1A. **(B)** WB of organoid samples after 7 days of OH-tamoxifen treatment; β-actin was used as loading control. **(C) CDK8/CDK19 KO organoids are counter-selected.** WB indicating the levels of CDK8, CDK19 and phospho-Stat1-S727 in organoids after 14 days of tamoxifen treatment. Two out of the three *Cdk8* $^{-/-}$*/Cdk19* $^{-/-}$ clones (clon 10 and clon 12) show a reappearance of the CDK8 protein: compare with Fig. 7B where proteins were extracted from the same samples, but one week earlier. (•) indicates the two clones where CDK8 protein is detected; this was observed only in organoids where double KO had been induced. **(D)** Phase contrast images of organoids before and after 6 days of OH-tamoxifen treatment. Scale bars, 150μm. **(E)** Quantification of organoid size at day 0 and 6, shown in D (mean + SD are shown). P-value, ordinary one-way ANOVA: (*) p ≤ 0.05, (***) p ≤ 0.001. **(F)** IHC staining of organoids (day 7 of OH-tamoxifen treatment) with Ki-67 antibody. Scale bars, 100μm. **(G)** Quantification of Ki-67 positive area (% of the total area of the organoids; mean + SD) in the four different genotypes presented in (F). Areas with positive Ki-67 signal were detected and quantified using QuPath and ImageJ programs. Adjusted p-values of ordinary one-way ANOVA followed by Tukey's multiple comparison test are indicated: (***) p-value ≤ 0.001; (**) p-values ≤ 0.01; (*) p-values ≤ 0.05; ns, not significant (p > 0.05).

Fig 8. Functional redundancy between CDK8 and CDK19 in regulation of gene expression
-Significant alteration of genes also modulated in intestinal KOs of the Cystic Fibrosis Transmembrane conductance Regulator (CFTR) in the *Cdk8*$^{-/-}$*/Cdk19*$^{-/-}$ KO

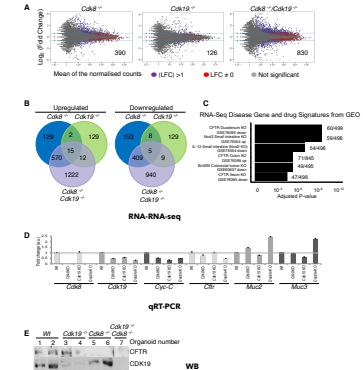

Fig. 8. (A) Dot plot analysis of differentially expressed genes (DEGs). Red dots: DEGs with p-value ≤ 0.05; purple dots: log_2 fold change (LFC) >1 or <-1, p-value ≤ 0.05; grey dots: not significant. Numbers inside plots indicate the number of genes deregulated more than 2-fold. **(B)** Venn diagrams indicating intersection of genes with altered expression in the indicated genotypes. **(C)** Gene set enrichment analysis (using Enrichr database) of highly deregulated genes in *Cdk8*$^{-/-}$*/Cdk19*$^{-/-}$ organoids. Manually curated signatures extracted from RNA-seq studies in GEO where gene expression was measured before and after drug treatment, gene perturbation or disease. **(D)** qRT-PCR analysis of indicated mRNA levels in Wt, *Cdk8*$^{-/-}$, *Cdk19*$^{-/-}$ and *Cdk8*$^{-/-}$*/Cdk19*$^{-/-}$ organoids. **(E)** WB of indicated proteins extracted from Wt, *Cdk8*$^{-/-}$, *Cdk19*$^{-/-}$ and *Cdk8*$^{-/-}$*/Cdk19*$^{-/-}$ organoids. Amidoblack was used as loading control.

Fig 9. CDK8 and CDK19 regulate the CFTR pathway in the small intestine.

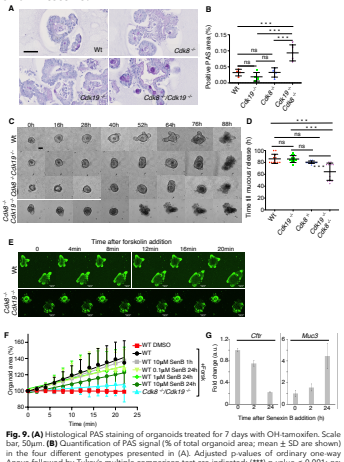

Fig. 9. (A) Histological PAS staining of organoids treated for 7 days with OH-tamoxifen. Scale bar, 50μm. **(B)** Quantification of PAS signal (% of total organoid area; mean ± SD are shown) in the four different genotypes presented in (A). Adjusted p-values of ordinary one-way Anova followed by Tukey's multiple comparison test are indicated: (***) p-value ≤ 0.001; ns: not significant (p > 0.05). **(C)** Representative phase contrast images of organoids at the indicated time points after 7 days of OH-tamoxifen treatment. Scale bar, 100 μm. **(D)** Quantification of the time needed for mucus release (observed as a dark staining in the center of the organoid; mean ± SD are shown). Adjusted p-values of ordinary one-way Anova followed by Tukey's multiple comparison test are indicated: (***) p-value ≤ 0.001; ns: not significant (p > 0.05); (n= 17 for Wt, n=11 for *Cdk8* $^{-/-}$, n=18 for *Cdk19* $^{-/-}$, n= 12 for *Cdk8* $^{-/-}$*/Cdk19* $^{-/-}$). **(E)** Fluorescence confocal microscopy images of Calcein green-labeled WT and *Cdk8*$^{-/-}$*/Cdk19*$^{-/-}$ organoids treated with forskolin. Scale bars, 100 μm. **(F)** Quantification of forskolin-induced swelling in WT organoids treated for 1hour or 24 hours with 0.1μM, 1μM or 10μM Senexin B (Sen8), as indicated, or double KO organoids; DMSO vehicle was used as control. The surface area of individual organoids at different time points relative to the area at t = 0 (100%) was measured (mean ± SD, n=8). Linear regression lines are shown. **(G)** qRT-PCR analysis of Cftr and Muc3 mRNA levels in WT organoids either not treated (t=0), or treated with 10μM Senexin B for 2 or 24 hrs.

Conclusions

-Our *in vivo* results support that ***Cdk8* has neither oncogenic nor strong tumour suppressor activity** in the mouse intestine.

-No critical role for CDK8 in RNA-PolII CTD phosphorylation

-**Mediator kinases are both functionally redundant** and largely dispensable for cell survival, proliferation, and differentiation, but may be essential for regulation of specific gene sets in particular cell types; in this case, the CFTR pathway in the intestinal epithelium.

-In the intestinal epithelium, cells devoid of both kinases have an increased tendency to become quiescent, implying that **CDK8 and CDK19 provide a growth advantage**.

-**Kinase activity of CDK8/19 controls CFTR pathway gene expression**. Double knockout organoids showed **increased mucin expression** and strong **accumulation of mucins in goblet cells**, coupled with a **precocious secretion of mucus**, as well as a **lack of forskolin-induced swelling**, which depends on CFTR, indicating that CDK8/19 regulate fluid and/or mucus homeostasis.

-Since we only observe an inhibition of forskolin induced swelling when the organoids are incubated during 24 hours in the presence of CDK8/19 inhibitor (Senexin B), and not after 1 hour of incubation, the **mechanism of action appears to be due to transcriptional downregulation of *Cftr*** and not to direct phosphorylation of CFTR.

-Identifying the mechanisms by which CDK8 and CDK19 affect expression of genes in the CFTR pathway will be important to better understand the pathophysiology of cystic fibrosis.

Sponsors